C. R. Palevol 17 (2018) 189–200

Contents lists available at ScienceDirect

Comptes Rendus Palevol

www.sciencedirect.com

General Palaeontology, Systematics and Evolution (Vertebrate Palaeontology)

The first French tragulid skull (Mammalia, Ruminantia, Tragulidae) and associated tragulid remains from the Middle Miocene of Contres (Loir-et-Cher, France)

Le premier crâne de Tragulidae français (Mammalia, Ruminantia) et les restes associés de Tragulidae du Miocène moyen de Contres (Loir-et-Cher, France)

Bastien Mennecart[a,b,*], Adrien de Perthuis[c], Gertrud E. Rössner[d,e], Jonathan A. Guzmán[d,e,f], Aude de Perthuis[c], Loïc Costeur[a]

[a] *Nathurhistorisches Museum Basel, Augustinergasse 2, 4001 Basel, Switzerland*
[b] *Nathurhistorisches Museum Wien, Burgring 7, 1010 Vienna, Austria*
[c] *27, rue des Papegaults, 41000 Blois, France*
[d] *SNSB–Bayerische Staatssammlung für Paläontologie und Geologie, Richard-Wagner-Strasse 10, 80333 München, Germany*
[e] *Department für Geo- und Umweltwissenschaften, Paläontologie und Geobiologie, and GeoBio-Center der Ludwig-Maximilians-Universität München, Richard-Wagner-Str. 10, 80333 München, Germany*
[f] *Departamento de Ciencias Básicas, Universidad de Concepción, Campus Los Ángeles, Chile*

ARTICLE INFO

Article history:
Received 6 June 2017
Accepted after revision 17 August 2017
Available online 22 November 2017

Handled by Lorenzo Rook

Keywords:
Comparative anatomy
Langhian
Inner ear
3D
Heterochrony

ABSTRACT

The Faluns Auger quarry (Contres, France) is famous for its Langhian mammal fauna (MN5) and tragulid remains have been identified as *Dorcatherium* sp. New excavations provided a fragmented skull of a tragulid, dental remains, and a metapodium which we describe here. Based on morphological and morphometrical characters, these specimens are attributed to *Dorcatherium crassum*. CT-scans provide insight in the petrosal bone and bony labyrinth. We prove intra-population variability of the p4 and intra-specific variability of the bony labyrinth. Nevertheless, we can demonstrate that the bony labyrinth is useful for systematics. Thus, we confirm the presence of *D. crassum* in the Pontlevoy–Thenay and Savigné-sur-Lathan Faluns Basins as reported already prior to our study. Yet, we cannot confirm evidence for *Dorcatherium naui*. *D. naui* specimens reported from these basins may belong to another species. *D. naui* should be absent from the Faluns before MN7, such as in the rest of Europe.

Mots clés :
Anatomie comparée
Langhien
Oreille interne
3D
Hétérochronie

RÉSUMÉ

La carrière à faluns dite « Auger » à Contres (France) est connue pour avoir fourni une faune de mammifères du Langhien (MN5), dont un Tragulidae, identifié comme *Dorcatherium* sp. Lors de nouvelles excavations, un crâne partiel de Tragulidae, ainsi que des restes dentaires et un métapode ont été découverts. Sur la base de caractères morphologiques et morphométriques, ces derniers sont attribués à *Dorcatherium crassum*. Le pétreux et le

* Corresponding author. Nathurhistorisches Museum Basel, Augustinergasse 2, 4001 Basel, Switzerland.
E-mail address: mennecartbastien@gmail.com (B. Mennecart).

https://doi.org/10.1016/j.crpv.2017.08.004
1631-0683/

labyrinthe osseux sont décrits. Il est mis en évidence qu'il existe une variabilité intrapopulationnelle de la p4, ainsi qu'une légère variabilité intraspécifique du labyrinthe osseux. Cependant, nous confirmons ici que cette structure interne peut être utilisée à des fins taxonomiques. *D. crassum* est déjà bien connu dans les bassins de Pontlevoy–Thenay et de Savigné-sur-Lathan. Nous soupçonnons cependant que les spécimens attribués à *D. naui* de ces bassins appartiennent à une autre espèce. *D. naui* est absent dans le reste de l'Europe avant MN7.

1. Introduction

The ruminant family Tragulidae, members of which commonly called chevrotains or mouse deer, includes the only living ruminant species that do not belong to the clade of the derived pecoran ruminants (Hassanin et al., 2012; Nowak, 1999). They possess only three fully formed stomach chambers, missing the omasum (Boas, 1890; Clauss & Rössner, 2014; Milne-Edwards, 1864; Nowak, 1999; Rössner, 2007) and are usually described as primitive (e.g., Métais & Vislobokova, 2007; Rössner, 2007). Their origin in the Paleogene and their early evolution remain uncertain due to a sporadic fossil record and extremely few species and genera known during this period (Mennecart & Vislobokova; Mennecart et al., 2011; Métais & Vislobokova, 2007; Métais et al., 2001; and references therein). In contrast, their Neogene fossil record is extensive in the Old World (e.g., Clauss & Rössner, 2014; Gentry et al., 1999, Rössner, 2007, Sánchez et al., 2015). Over 30 species have been described in the Miocene, mainly from Asia (Kostopoulos & Sen, 2016; Rössner, 2007). In Europe, their Neogene fossil record is exclusively affiliated to the genus *Dorcatherium* with seven different species from the latest early Miocene to the latest Miocene (*D. guntianum*, *D. crassum*, *D. vindebonense*, *D. peneckei*, *D. naui*, *D. puyhauberti*, and *D. jourdani*; Aiglstorfer et al., 2014; Rössner, 2007; Rössner & Heissig, 2013). However, several authors (e.g., Rössner & Heissig, 2013; Sánchez et al., 2015) recognize that *Dorcatherium* is most probably a polyphyletic genus.

European skull material, sufficiently well-preserved to allow α-taxonomic assessment, is currently only known from Germany (*D. naui* skulls from Eppelsheim described Kaup, 1839, the undescribed *Dorcatherium* skull from Steinheim am Albuch figured in Gentry et al., 1999: 23.3 [there affiliated to *D. naui*; but affiliated to *D. guntianum* in Rössner & Heissig, 2013 online resource 2 and to *D. crassum* in Aiglstorfer et al., 2014], and the superficially described *D. crassum* skull from Thierhaupten, Seehuber, 2015). Although, French localities also yielded an abundant fossil record for *Dorcatherium*, from none of those a skull or partial skull has been reported up to now, not even from the outstanding Sansan fossil site (Gers), which is the type locality for *D. crassum* (Morales et al., 2012). Yet,

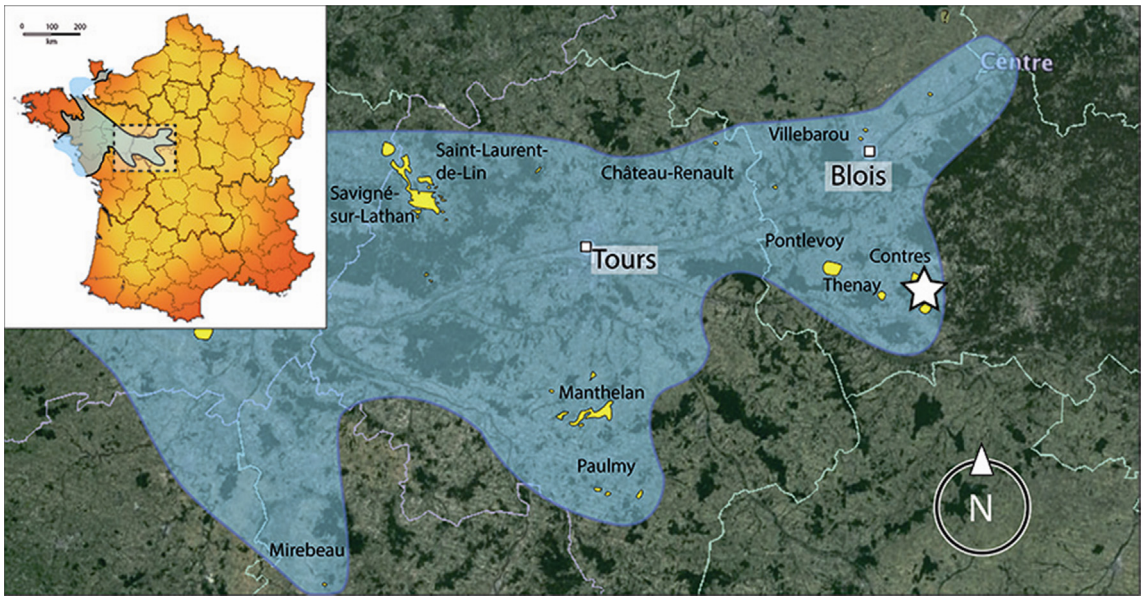

Fig. 1. Location of the Faluns formation and outline of the Falun Sea (France). The yellow patches correspond to Faluns deposits. The light blue represents the maximum of extension of the Langhian Sea. The white star locates the Contres locality. The figure has been modified from Dubied et al. (2017).
Fig. 1. Localisation de la formation des Faluns et contour de la mer des Faluns (France). Les zones jaunes correspondent aux dépôts de faluns. La zone bleutée représente l'extension maximale de la mer Langhienne. L'étoile blanche localise Contres. Cette figure a été modifiée à partir de Dubied et al. (2017).

since *D. crassum* is the only tragulid species known from Sansan (Mennecart & Costeur, 2016b; Morales et al., 2012) attributed an isolated petrosal bone from Sansan to it (see Mennecart & Costeur, 2016c for access to 3D reconstruction).

Here we provide the description of a partial skull and other dental and postcranial remains from the Auger quarry area in Contres (Loir-et-Cher, Pontlevoy–Thenay Basin) ca. 200 km south-southwest of Paris (Fig. 1) attributed to *D. crassum*. This is the first largely preserved tragulid skull known from France and the first extensive description for a skull of *D. crassum*.

2. Material & methods

2.1. Geological setting

Castillo et al. (2006) and Gagnaison et al. (2006) already mentioned some remains of *Dorcatherium* sp. from the Auger quarry. The site was exploited for fossils from 1995 to 1997 (Gagnaison et al., 2006). It is now totally exploited and the locality is sealed, but from 2012 to 2016, a last excavation led by two of us provided the new *D. crassum* material described here. The fossils have been discovered in an estuarine layer overlaying the fully marine Falun deposits (Castillo et al., 2006). The abundant fauna (more than 1.000 specimens discovered during two several-weeks lasting excavation campaigns) permits an assignation to the sub-mammal zone MN5b, ca. 15Ma (Castillo et al., 2006).

2.2. Material

The original specimens are currently stored in the private collection of A. de Perthuis. These specimens will be given to a natural history museum and all the data about the location of these fossils (currently in the collection or to be collected in the future) will be provided to the Naturhistorisches Museum Basel, along with casts to facilitate management of the collection. Casts and digital specimens are kept in the Naturhistorisches Museum Basel (Switzerland). Digital 3D data of the skull (AP2014.0715 and cast NMB Fa.213.abg), its isolated right petrosal, and the reconstructed left bony labyrinth are freely accessible on the MorphoMuseum web site (Mennecart et al., online). Specimens of recent tragulids for comparison (*Hyemoschus*, *Moschiola*, and *Tragulus*) are stored in the Naturhistorisches Museum Basel.

To access the bony labyrinth and create a virtual model of the skull (3D data made of the maxilla and associated teeth, the basicranium, excepted for the isolated part of basisphenoid and basioccipital, and the skull roof only), the specimens were scanned using high-resolution X-ray computed tomography (Phoenix Nanotom, GE, at the Biomaterials Science Centre of the University of Basel, Switzerland). Scanning resolution was 55 μm for the entire skull and 35 μm for a second scan focusing on the ear region. A total of 1440 equiangular radiographs were taken over 360° using an accelerating voltage of 170 kV and a beam current of 30 mA. Segmentation of the specimen was carried out with the AVIZO 9.0 software (Visualization Sciences Group).

2.3. Terminology

Terminology for skull elements follows Baron (1999), for the petrosal bone O'Leary (2010), for the bony labyrinth Ekdale (2013), for tooth crown elements Bärmann & Rössner (2011) (see Fig. 2) and for postcranial elements Köhler (1993). Measurements have been taken with a calliper (0.1 mm precision).

2.4. Abbreviations

NMB: Naturhistorisches Museum Basel; AP: collection A. de Perthuis; p: lower premolar; m: lower molar; P: upper premolar; M: upper molar; Mt: metatarsal bone.

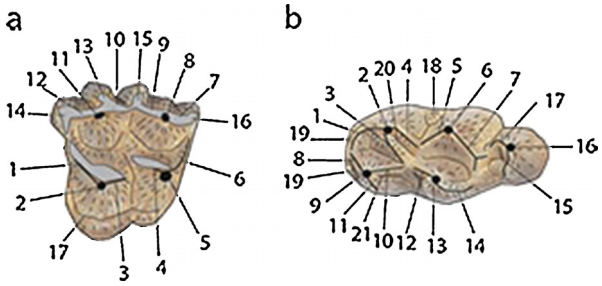

Fig. 2. Dental nomenclature (mainly based on Bärmann & Rössner, 2011). **a**, upper molars: **1**, preprotocrista; **2**, protocone; **3**, postprotocrista; **4**, premetaconulecrista; **5**, metaconule; **6**, postmetaconulecrista; **7**, postmetacrista; **8**, metacone; **9**, premetacrista; **10**, postparacrista; **11**, paracone; **12**, preparacrista; **13**, paracone rib; **14**, parastyle; **15**, mesostyle; **16**, metastyle; **17**, cingulum; **b**, lower molars: **1**, preprotocristid; **2**, protoconid; **3**, internal postprotocristid; **4**, external postprotocristid; **5**, prehypocristid; **6**, hypoconid; **7**, posthypocristid; **8**, premetacristid; **9**, metaconid; **10**, internal postmetacristid; **11**, external postmetacristid; **12** preentocristid; **13**, entoconid; **14**, postentocristid; **15** posthypoconulidcristid; **16**, hypoconulid; **17**, prehypoconulidcristid; **18**, ectostylid; **19**, anterior cingulid; 20, *Tragulus* fold; 21, *Dorcatherium* fold.

Fig. 2. Nomenclature dentaire (modifiée d'après Bärmann & Rössner, 2011). **a**, molaires supérieures : **1**, préprotocrista ; **2**, protocone ; **3**, postprotocrista ; **4**, prémétaconulecrista ; **5**, métaconule ; **6**, postmétaconulecrista ; **7**, postmétacrista ; **8**, métacone ; **9**, prémétacrista ; **10**, postparacrista ; **11**, paracone ; **12**, préparacrista ; **13**, côte du paracone ; **14**, parastyle ; **15**, mésostyle ; **16**, métastyle ; **17**, cingulum ; **b**, molaires inférieures: **1**, préprotocristide ; **2**, protoconide ; **3**, postprotocristide interne ; **4**, postprotocristide externe ; **5**, préhypocristide ; **6**, hypoconide ; **7**, posthypocristide ; **8**, prémétacristide ; **9**, métaconide ; **10**, postmétacristide interne ; **11**, postmétacristide externe ; **12** préentocristide ; **13**, entoconide ; **14**, postentocristide ; **15** posthypoconulidcristide ; **16**, hypoconulide ; **17**, préhypoconulidcristide ; **18**, ectostylide ; **19**, cingulide antérieur ; 20, *Tragulus* fold ; 21, *Dorcatherium* fold.

3. Systematic Paleontology and description

Order: Artiodactyla Owen, 1848
Suborder: Ruminantia Scopoli, 1777
Infraorder: Tragulina Flower, 1883
Family: Tragulidae Milne Edwards, 1864
Genus ***Dorcatherium*** Kaup, 1833
Dorcatherium crassum (Lartet, 1839)

Figs. 2–6 Tables 1–3.

Referred specimens. AP2014.0715 (NMB Fa.213.abg digital copy, see Mennecart et al., 2017, and 3D print) fragmented skull containing the basicranium represented by isolated basisphenoid and basioccipital, the skull roof, and the left maxilla with P4–M3 mainly (Figs. 3 and 4); AP2013.0135 right maxilla with P4–M3; AP2015.0134 right maxilla with M1–M3; AP2012.0130 (NMB Fa.214.abg cast) right corpus mandibulae with p3–m3; AP2014.0129 (NMB Fa.215.abg cast) right corpus mandibulae with p2–m3 (Fig. 5.1); AP2015.0131 left m2–m3; AP2015.0133 fragmented right corpus mandibulae with p3–m1; AP2013.0132 fragmented right corpus mandibulae with p3 and alveolus of two rooted p2; AP2015.0128 (NMB Fa.216.abg cast) left Mt III–IV (Fig. 5.2).

Skull. The skull is highly fragmented but some delicate structures (e.g., eye socket, bulla, and probably vomer) are partly conserved. The best-preserved bones are from the skull roof (frontals, parietals, squamosals, proximal part of the nasals, and the left maxilla bone), and the basicranium (basisphenoid, and the occipital). The naso-frontal suture is W-shaped, with the posterior part of it, reaching the level of the centre of the orbits in dorsal view. The frontals form an elongated bone extension going between the nasal bones. In living species, the nasal and frontals suture is also not straight, but is farther anterior of the orbits and relatively flat, although a little variation is observed within a species (pers. obs. on *Tragulus kanchil* and *Hyemoschus aquaticus*) with individuals fluctuating from flat to convex shape nasal bone. The supraorbital foramen is larger than in living the tragulids. It is separated from the deep supraorbital groove by a robust bony bridge. These structures are slender in living tragulids (Rössner, 2007: fig. 16.3A; pers. obs.; Smit-van Dort, 1989: fig. 1). The orbit is well-rounded such as in *D. naui* from Eppelsheim and *D. crassum* from Steinheim am Albuch. However, this character is highly variable in living tragulids, being rounded, rectangular, or even more triangular. The postorbital bar of the frontal process is broad on the orbital face, such as in the Thierhaupten specimen. In living tragulids, this part is more slender. The sagittal crest is well-developed separating into the left and the right parietofrontal suture in the middle of the braincase with an angle of 90°, such as in the Thierhaupten specimen. It is a wide ridge and passes at the dorsocaudal skull edge to the well-developed nuchal crest forming the framing external crests of the occipital. Among the living tragulids, only *Hyemoschus* possesses such structures, but more weakly developed. In *Tragulus* and *Moschiola*, the sagittal crests are incipient and the nuchal crest is weak to absent (Rössner, 2007: fig. 16.3A; Smit-van Dort, 1989: fig. 1). Contrary to *Hyemoschus*, no external occipital crest is observed in the *Doractherium* specimen described here. Similar to *Hyemoschus*, the dorsal part of the occipital condyles is somewhat detached from the dorsal condylar fossa area. The two nuchal tubercles are well-developed, while they are absent in living taxa. The jugular processes, even if broken, are more similar in shape to *Hyemoschus* than to the other living tragulid genera *Moschiola* and *Tragulus* in being more profiled and relatively larger. It is even stockier than in *Hyemoschus* and possesses a tuberosity.

Petrosal bone. The petrosal bone has a rather broad epitympanic wing with a pointed apex, it is more elongated than in *Tragulus* and *Moschiola* (Mennecart & Costeur, 2016b). The promontorium on the ventrolateral side is tubular in shape with a broad posterior part (Fig. 4.a1). It has a flat convex surface like the petrosal bone of *D. crassum* from Sansan (Mennecart & Costeur, 2016b) and does not show the two distinct convexities seen in *Tragulus* (O'Leary, 2010). There is no apparent transpromontorial sulcus as already observed on all living tragulids and on *D. crassum* from Sansan (O'Leary, 2010; Mennecart & Costeur, 2016b). The fossa for the tensor tympani muscle is large as in *Hyemoschus* and has a quadratic shape that becomes more elongated anteriorly. It does not excavate into the tegmen tympani. It occupies slightly more than half the size of the promontorium, much of its anterior part. The crista interfenestralis between the fenestrae vestibuli and cochleae is broad and both fenestrae have about the same size. A small but deep fossa for the attachment of the stapedial muscle is visible directly posteriorly to the fenestra vestibuli. The facial sulcus is nor very broad neither very deeply impressed. No protruding articulations to the medial or posterior bulla are visible, but this may be due to the 3D reconstruction. In contrast the articulation to the anterior bulla is well visible on the ventrolateral side next to the anterior process of the tegmen tympani.

The dorsomedial side shows a knob (Fig. 4.a1), again as in *Hyemoschus* and unlike in *Tragulus* or *Moschiola*. The hiatus fallopii sits within a subcentral elongate slit of the tegmen tympani. The tegmen tympani extends anteriorly almost up to the level of the most anterior part of the promontorium, being slightly smaller than on the specimen from Sansan. It has a blunt apex. No basicapsular groove is visible recalling the situation in Sansan. It is also hard to observe on the three living tragulid genera as shown by Mennecart & Costeur (2016b). The subarcuate fossa is rather shallow. The opening of the vestibular aqueduct sits centrally posterior to the internal acoustic meatus as on the specimen from Sansan. The opening for the cochlear aqueduct is located more anteriorly on the ventromedial side at the level of the internal acoustic meatus and it sits on the dorsal extension of the ventromedial side. The mastoid region is wedge-like as in living and fossil tragulids where it is known and as in ruminants in general (Mennecart & Costeur, 2016b; O'Leary, 2010).

Bony labyrinth. The bony labyrinth is very similar to that of *D. crassum* described in Mennecart & Costeur (2016b). Linear and volumetric measurements are given in Table 1. The cochlea has three turns (Fig. 4.b2). It is massive, compact and tall because of the large number of turns compared with other ruminants (Costeur, 2014). The aspect ratio (total height divided by total width) is 0.55,

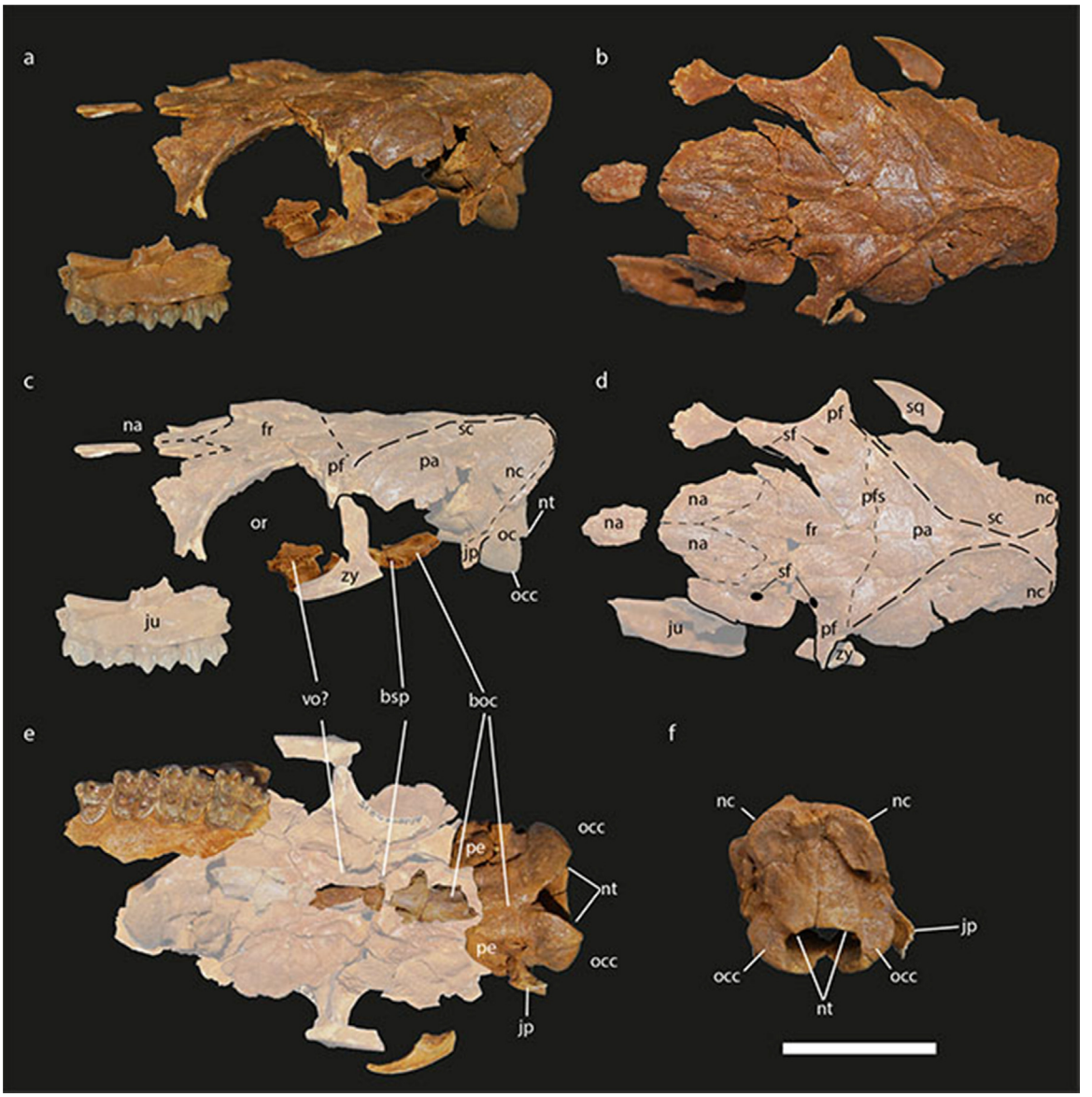

Fig. 3. Skull of *Dorcatherium crassum* from Contres (original specimen AP2014.0715 and digital copy NMB Fa.213.abg). **a** & **c** lateral (left), **b** & **d** dorsal, **e** ventral, **f** posterior view. Abbreviations: **boc**, basioccipital; **bsp**, basisphenoid; **fr**, frontal; **jp**, jugular process; **mx**, maxilla; **na**, nasal; **nc**, nuchal crest; **nt**, nuchal tubercule; **oc**, occipital condyle; **or**, orbit; **pa**, parietal; **pe**, petrosal; **pf**, postorbital bar of the frontal process; **pfs**, parietofrontal suture; **sc**, sagittal crest; **sf**, supraorbital foramen; **sq**, squamosal; **vo**?, vomer?; **zy**, zygomatic. The scale bar is 5 cm.

Fig. 3. Crâne de *Dorcatherium crassum* de Contres (spécimen original AP2014.0715 et copie digitale NMB Fa.213.abg). **1** Morphologie externe du crâne en vues **1a & c** latérale (gauche), **1b & d** dorsale, **1e** ventrale, **1f** postérieure. Abréviations : **boc**, basioccipital ; **bsp**, basisphénoïde ; **fr**, frontal ; **jp**, processus jugulaire ; **mx**, maxillaire ; **na**, nasal ; **nc**, crête nuchale ; **nt**, tubercule nuchal ; **oc**, condyle occipital ; **or**, orbite ; **pa**, pariétal ; **pe**, os pétreux ; **pf**, barre postorbitale du processus frontal ; **pfs**, suture pariétofrontale ; **sc**, crête sagittale ; **sf**, foramen supraorbital ; **sq**, squamosal ; **vo** ?, vomer ? ; **zy**, zygomatique. La barre d'échelle est de 5 cm.

slightly below those of the living tragulids and of *D. crassum* from Sansan (Mennecart & Costeur, 2016b) but in the range of high cochleas. The cochlear spiral is tight and only half of the basal turn is detached from the rest of the cochlea. The cochlear aqueduct is enlarged, with a flattened diameter. The secondary bony lamina is well visible over most of the basal turn, so apparently longer than in *D. crassum* from Sansan, but preservation could play a role here since the specimen from Sansan was recrystallized (Mennecart & Costeur, 2016b) and thus less well preserved than here. The fenestra cochleae is rounded in shape and faces laterally. On the vestibule, both the sacculus and utriculus are well defined (Fig. 4.b1) such as on the Sansan specimen. The fenestra vestibuli is large and oval in shape, with a stapedial ratio of 1.62, exactly like *D. crassum* from Sansan. The anterior semicircular canal is the most dorsally expanded canal; it expands largely above the level of the common crus, as for the posterior semicircular canal but to a lesser extent

for the latter. The common crus is less indented and longer than on the specimen from Sansan (Mennecart & Costeur, 2016b) but such a variation was observed on the living *Tragulus kanchil* (Mennecart & Costeur, 2016a). The lateral semicircular canal is straight. It branches dorsally above the posterior ampulla, in the vestibule between the latter and the base of the common crus, a typical feature of Tragulidae. In addition and in line with previous observations on extinct and extant tragulids, the lateral semicircular canal extends beyond the plane of the posterior semicircular canal in dorsal or lateral view. The vestibular aqueduct is a thin canal detached from the common crus over most of its course, as in the Sansan specimen. It originates in the vestibule at the base of the common crus but anteriorly. It runs parallel to the midline of the common crus along its course and is thus not curved; it extends above the end of the common crus dorsally, less so on this specimen than on that of Sansan because the common crus is longer here. The endolymphatic sac at the end of the vestibular aqueduct is large and broad, triangular in shape with a broad base, larger than on the Sansan specimen, but this feature is ontogenetically variable in size.

Upper dentition. The enamel is wrinkled. The cusps are bunoselenomorph. The triangular P4 possesses only one labial cone with an extremely little developed labial rib. The worn anterolabial crista joins the bulbous base of the anterior style that has a crescent shape and forms the anterolabial edge of the tooth. This style is well-developed. The anterolingual crista is straight and links the anterior style to the medial and crescentic lingual cone. The posterolingual crista is short, stopping at the level of the middle of the posterolabial crista. The posterolabial crista is a little concave and joins the posterolabial edge of the tooth. There is no marked posterior style. The lingual cingulum is well marked from the anterolingual edge of the tooth to its posterolabial edge. The upper molars increase in overall size from M1 to M3 (Table 2). They are relatively square in shape. The paracone rib, as well as mesostyle and parastyle are well-developed in contrast to the weak metacone rib. They increase in size from M1 to M3 as well. Paracone and metacone are almost in line. Labial cristae are short and straight. The metastyle is only present on M3. The anterior fossa is widely opened due to a postprotocrista posteriorly oriented. The straight preprotocrista is interrupted by the anterolabial edge of the anterior tooth. The metaconule is V-shaped. The premetaconulecrista is straight and ends

Table 1
Measurements of the bony labyrinth of *D. crassum* from the Auger quarry (Contres, France) with comparative measurements from the literature (Mennecart & Costeur, 2016b). **ASC**: anterior semicircular canal; **LSC**: lateral semicircular canal; **PSC**: posterior semicircular canal.
Tableau 1
Dimensions du labyrinthe osseux de *D. crassum* de la carrière Auger (Contres, France) et comparaison avec les données de la littérature (Mennecart & Costeur, 2016b). **ASC** : canal semi-circulaire antérieur ; **LSC** : canal semi-circulaire latéral ; **PSC** : canal semi-circulaire postérieur.

	AP2014.0715	NMB San.15053
	Contres MN5	Sansan MN6
Number of cochlear turns	3	3
Volume (mm^3)	83.2	67.6
Stapedial ratio	1.62	1.62
Cochlear aspect ratio	0.55	0.63
ASC height (mm)	4.76	4.71
ASC width (mm)	4.54	4.32
PSC height (mm)	4.21	4.15
PSC width (mm)	4.7	4.05
LSC length (mm)	3.93	3.82
LSC width (mm)	3.43	4.18
Angle ASC–PSC	77°	84°
Angle ASC–LSC	73°	73°
Angle PSC–LSC	80°	85°

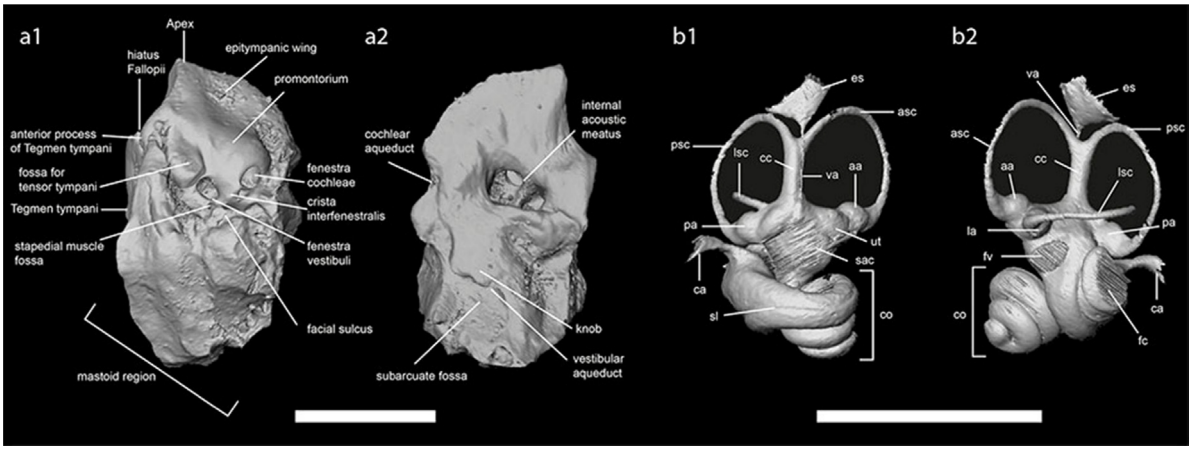

Fig. 4. a right petrosal bone and **b** left bony labyrinth of *Dorcatherium crassum* from Contres (original specimen AP2014.0715 and digital copy NMB Fa.213.abg): **a1** and **b2** ventrolateral view, **a2** and **b1** dorsomedial view. Scale bare is 1 cm. Abbreviations: **aa**, asc ampulla; **asc**, anterior semi-circular canal; **ca**, cochlear aqueduct; **cc**, common crus; **co**, cochlea; **es**, endolymphatic sac; **fc**, *fenestra cochleae*; **fv**, *fenestra vestibuli*; **la**, lsc ampulla; **lsc**, lateral semi-circular canal; **pa**, psc ampulla; **psc**, posterior semi-circular canal; **sac**, *sacculus*; **sl**, secondary bony lamina; **ut**, *utriculus*; **va**, vestibular aqueduct.
Fig. 4. Os pétreux droit (**a**) et labyrinthe osseux gauche (**b**) du crâne de *Dorcatherium crassum* de Contres (spécimen original AP2014.0715 et copie digitale NMB Fa.213.abg) : **a1** et **b2** en vue ventro-latérale et **a2** et **b1** en vue dorso-médiale. La barre d'échelle est de 1 cm. Abréviations : **aa**, ampoule asc ; **asc**, canal semi-circulaire antérieur ; **ca**, aqueduc cochléaire ; **cc**, crus commun ; **co**, cochlée ; **es**, sac endolymphatique ; **fc**, *fenestra cochleae* ; **fv**, *fenestra vestibuli* ; **la**, ampoule lsc ; **lsc**, canal semi-circulaire latéral ; **pa**, ampoule psc ; **psc**, canal semi-circulaire postérieur ; **sac**, *sacculus* ; **sl**, lamina osseuse secondaire ; **ut**, *utriculus* ; **va**, aqueduc vestibulaire.

in between the paracone and metacone. The postmetaconulecrista is incomplete on M1 and does not reach the posterolabial edge of the tooth. The posterior cingulum is weak on M1, is weaker on M2, and is absent on M3. The anterolingual cingulum becomes more and more pronounced from M1 to M3. There is no entostyle or accessory fold.

Mandible. The corpus mandibulae gradually enlarges in height from rostral to caudal below the teeth until the concavity of the incisura vasorum starts. This incisura is not marked, but smoothed. The diastema starts right in front of the p2, similarly to the symphysis. The small and oval mandibular foramen is at the level of the tooth row. The two mental foramina are on the diastema and form an elongated fissure since they are connected.

Lower dentition. The lower premolars are more or less of the same size (Table 2). The p2 and p3 have a similar shape. These teeth are composed of three main conids aligned in the axis of the tooth. The mesolabial conid is central and the highest conid in all the premolars. All the cristids are straight, the laterally compressed anterior conid being anteriorly oriented in p2 and p3. The posterolabial conid bears a weakly developed curved posterior stylid that forms the posterolabial edge and the posterior part of the p2 and p3. The p3 differs from p2 in having a minute posterolingual conid absent on the other tooth. The p4 bears a posteriorly oriented transverse cristid. The posterior stylid is big and partly closes the steep-sided posterior valley between the transverse cristid and the posterolabial cristid. The anterior part of the p4 may bear an anterior stylid (AP2014.0.129) or not (AP2013.0130). The molars are bunoselenodont with a bulky lingual wall. They increase in size from m1 to m3. The preprotocristid is highly curved and joins the premetacristid on the anterior part

Table 2
Dental measurements (maximal length and width respectively in mm) of *D. crassum* from the Auger quarry (Contres, France) with comparative material from the literature (Morales et al., 2012; Rössner, 2010; Seehuber, 2015). Thierhaupten tooth averages are based on left and right dentition of the skull.
Tableau 2
Dimensions des dents (longueur et largeur maximales respectivement en mm) de *D. crassum* de la carrière Auger (Contres, France) et comparaison avec les données de la littérature (Morales et al., 2012 ; Rössner, 2010 ; Seehuber, 2015). Les tailles moyennes pour le spécimen de Thierhaupten sont basées sur les deux rangées dentaires du crâne.

	AP2012.0130 Contres MN5		AP2014.0129 Contres MN5		AP2015.0131 Contres MN5	
p2	–	–	11.3	4.4	–	–
p3	11.8	5.0	11.5	5.1	–	–
p4	10.6	5.5	11.5	5.8	–	–
m1	10.5	7.0	10.4	7.5	–	–
m2	11.4	8.1	12.6	8.5	12.1	8.7
m3	18.7	9.2	19.5	9.0	–	9.2

	AP2015.0133 Contres MN5		AP2013.0132 Contres MN5	
p2	–	–	–	–
p3	12.2	4.5	12.9	4.6
p4	11.1	5.4	–	–
m1	11.3	7.5	–	–
m2	–	–	–	–
m3	–	–	–	–

	AP2014.0715 Contres MN5		AP2013.135 Contres MN5		AP2015.0134 Contres MN5	
P4	9.1	10.0	9.2	10.6	–	–
M1	10.6	11.6	11.1	12.0	11.1	12.1
M2	12.1	13.4	12.5	13.8	12.0	13.7
M3	13.0	13.7	13.5	14.3	13.2	14.4

	Seehuber, 2015 (Thierhaupten MN5)		Morales et al., 2012 (Sansan MN6)		Rössner, 2010 (Sandelzhausen MN5)	
	Average	Average	Average	Average	Min–max	Min–max
p2	–	–	10.9	4.4	10.6–11.5	4.2–5.5
p3	–	–	10.5	4.6	11.3–12.5	4.0–5.2
p4	–	–	10.0	5.3	10.8–13.0	5.2–6.0
m1	–	–	9.5	7.4	10.5–11.9	6.3–8.5
m2	–	–	10.1	8.8	11.0–14.0	7.4–10.0
m3	–	–	17.2	8.8	17.5–20.9	7.9–10.2
P2	13.0	6.4	13.2	6.3	13.0	6.6
P3	6.6	8.0	11.3	7.4	11.0	7.5
P4	9.8	10.8	9.1	10.0	10.0	10.0–11.9
M1	10.1	11.6	10.3	11.8	10.0–10.3	11.0–11.1
M2	11.3	13.1	11.9	13.9	11.1–12.3	12.8–14.0
M3	12.5	14.3	13.3	14.7	12.0–12.7	14.1–14.5

Fig. 5. Dental remains and postcranial bones of *Dorcatherium crassum* from Contres. **1** Right corpus mandibulae with the tooth row p2–m3 (original specimen AP2014.0129 and cast NMB Fa.215.abg) in **1a** labial, **1b** occlusal, and **1c** lingual views; left Mt III-IV (original specimen AP2015.0128 and cast NMB Fa.216.abg) in **2a** plantar, **2b** medial, **2c** dorsal, **2d** proximal, and **2e** distal views. The scale bar is 5 cm.
Fig. 5. Restes dentaires et os postcrâniens de *Dorcatherium crassum* de Contres. **1** Corpus mandibulae droit avec la rangée dentaire p2–m3 (spécimen original AP2014.0129 et moulage NMB Fa.215.abg) en vues **1a** labiale, **1b** occlusale, et **1c** linguale; Mt III-IV gauche (spécimen original AP2015.0128 et moulage NMB Fa.216.abg) en vues **2a** plantaire, **2b** médiale, **2c** dorsale, **2d** proximale et **2e** distale. La barre d'échelle est de 5 cm.

of the teeth. The other cristids are straight. The external postprotocristid joins the prehypocristid, while the internal postprotocristid fuses with the internal postmetacristid forming a "*Tragulus* fold". The external postmetacristid forms a true "*Dorcatherium* fold". The association of the "*Tragulus* fold" with the "*Dorcatherium* fold" forms the typical tragulid "M-structure". The entoconid is a little oblique, giving birth to a straight preentocrisitd that fuses with the distal part of the internal postmetacristid and postprotocristid in the centre of the occlusal area. The lingual entoconid ridge on the apex of the enctonid is absent on m1, tiny on m2, and small on m3. The postentocristid is short and does not reach the base of the posthypoconidcristid. Since the entoconid is very bulky, there is an internal groove between this cristid and the cuspid. The relatively high hypoconulid forms the posterolabial corner of the m3. The prehypoconulicristid fuses with the base of the posthypocristid while the oblique back fossa of the m3 is opened lingually. The ectostylid is weakly developed and the posterior ectostylid is absent. The anterior cingulid is increasingly developed from m1 to m3. There is neither a metastylid nor an entostylid.

Postcranial bones. The metatarsal bones III and IV are fully fused in AP2015.0128 (size data are provided in Table 3). The proximo-plantar area is damaged. The distal part is enlarged compared to the diaphysis and keels articulating with the first phalanges are absent dorsally and distally. 22 mm above the distal end of the bones, an elongate, enlarged and deep metacarpal sulcus runs from dorsal to plantar. There are no additional crests on the edge of the sulcus (similar to the fig. 19 of Köhler, 1993). From the lateral view, the distal articular surfaces are flattened. The verticilli are weak and continue on the plantar surface in straight lines forming no real separation between the keels and the metaphysis. At the level of the greatest transverse diameter, there is a crest separating the rounded dorsal part of the bones from the flattened plantar one. The metatarsal bones are somewhat concave distally on the plantar side and convex on the dorsal side. On the proximal part of the bones, there is a longish furrow for the extensor tendon. On the plantar side, there are two small furrows which formed the articular areas with Mt II and Mt V. The proximal view does not allow a precise description of the articular surfaces. Nevertheless, it seems that the cuneiform articular surface of Mt III is half-moon shaped. The Mt III extends farther proximad, while the Mt IV extends farther distad. The metatarsal bones of *D. crassum* described herein are characteristic of Köhler's type A2 (wooded, very humid to semiaquatic habitat; Köhler, 1993).

4. Comparison and discussion

4.1. Taxonomical attribution

The p4, lacking a mesolingual conid, is typical for Tragulina (Mennecart, 2012; Mennecart et al., 2011). Moreover, the "M-structure" formed by the presence of a "*Tragulus*" fold and a "*Dorcatherium*" fold and the general shape of the bony labyrinth including the insertion of the lateral canal in the vestibule high dorsally between the posterior ampulla and the common crus associated with the high number of cochlear turns are unique to members of

Table 3
Measurements of metatarsal bones (in mm) of *D. crassum* from the Auger quarry (Contres, France) with comparative measurements from the literature (Morales et al., 2012; Rössner, 2010). **DAP**: dorso-palmar diameter; **dist**: distal; **DT**: latero-medial diameter; **prox**: proximal.
Tableau 3
Dimensions des métatarses (en mm) de *D. crassum* de la carrière Auger (Contres, France) et comparaison avec les données de la littérature Morales et al., 2012 ; Rössner, 2010). **DAP** : diamètre dorso-palmaire ; **dist** : distal ; **DT** : diamètre latéro-médial ; **prox** : proximal.

Mt III–IV	Morales et al., 2012	Rössner, 2010	AP2015.0128
	(Sansan Mn6)Average	(Sandelzhausen)	
Length	92.8	96	93.6
DT prox	20.1	–	20.5
DAP prox	18	–	–
DT dist	25.4	–	24.6
DAP dist	14.5	–	14.7

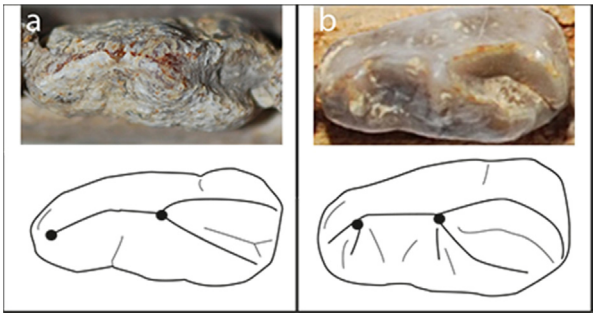

Fig. 6. Variation in the p4 in *D. crassum* from the Auger quarry (Contres, France). **a**, AP2012.0130 (NMB Fa.214.abg cast); **b**, AP2014.0129 (NMB Fa.215.abg cast).
Fig. 6. Variation de la p4 chez *D. crassum* de la carrière Auger (Contres, France). **a**, AP2012.0130 (NMB Fa.214.abg cast); **b**, AP2014.0129 (NMB Fa.215.abg cast).

Tragulidae (Costeur, 2014; Costeur et al., 2014; Gentry et al., 1999; Mennecart & Costeur, 2016a, 2016b; Mennecart et al., 2011; Mennecart & Métais, 2015; Métais & Vislobokova, 2007). All European tragulid species known are attributed to *Dorcatherium* (e.g., Aiglstorfer et al., 2014; Gentry et al., 1999; Rössner, 2007, Rössner & Heissig, 2013). Van der Made (1996) mentioned a cf. *Dorcabune anthracotherioides* in the late Miocene of Kastellios K east (Crete, Greece). *Dorcatherium* clearly differs from Paleogene members of Tragulidae (*Archaeotragulus* and *Iberomeryx*) and the Neogene *Afrotragulus* notably in size (being much larger), the proportional length of the diastema, and the more brachydont condition (Mennecart, 2012; Mennecart et al., 2011; Métais et al., 2001; Sánchez et al., 2010). But most probably *Dorcatherium* is a polyphyletic genus (Rössner & Heissig, 2013; Sánchez et al., 2015) and thorough revision is needed (Rössner, 2007). Two main "lineages" or "ecomorphotypes" can be separated among European *Dorcatherium*: the bunoselenodont (*D. crassum*, *D. vindebonense*, *D. peneckei*) and the selenodont (*D. guntianum*, *D. naui*, *D. puyhauberti*, and *D. jourdani*) (Aiglstorfer et al., 2014; Fahlbusch, 1985; Morales et al., 2012; Mottl, 1961; Rössner, 2007; Rössner & Heissig, 2013). Moreover, contrary to Mennecart et al. (2011), we want to point out here that not all species attributed to *Dorcatherium* do possess a p1. The presence or absence of a p1 may vary within a population (e.g., Aiglstorfer et al., 2014). Nevertheless, *D. vindebonense* and *D. naui* very often possess a p1 (Aiglstorfer et al., 2014; Alba et al., 2011; Ginsburg & Mornand, 1986 for *D. naui*), while *D. crassum* mostly lacks this tooth, as it is part of its diagnosis (Aiglstorfer et al., 2014; Ginsburg & Mornand, 1986; Morales et al., 2012; but see Rössner, 2010: fig. 1N and Gentry et al., 1999: fig. 23.2, there mistakenly named *D. naui*). The two mental foramina are located at the level of the diastema and form an elongated fissure since they are connected in *D. crassum* (Morales et al., 2012). They are well separated in *D. naui* (Aiglstorfer et al., 2014) being placed below p1 and p2 and below the middle of the diastema. Aiglstorfer et al. (2014) noticed that the more bunodont *Dorcatherium* species (*D. crassum* and *D. vindebonense*) possess simpler p4 structures than *D. naui* and *D. guntianum*, which have a complex structure in the posterior valley. Moreover, in the selendont *Dorcatherium* species (*D. naui*. and *D. guntianum*), the third lobe of the m3 is turned to labial, while in the bunodont ones (*D. crassum*, *D. vindebonense*, and *D. peneckei*), the third lobe is not turned as much (Aiglstorfer et al., 2014). The structure of the p4 and m3 of the studied specimens supports that they belong to the bunoselenodont "lineage".

Additionally, *Dorcatherium* species may also be separated by size (Aiglstorfer et al., 2014; Alba et al., 2011; Fahlbusch, 1985; Morales et al., 2012; Rössner & Heissig, 2013). Within *Dorcatherium*, *D. vindebonense*, and *D. peneckei* remains are large to very large, while those of *D. guntianum* and *D. puyhauberti* are small. Those of *D. naui*, *D. jourdani*, and *D. crassum* are medium-sized. The size dimensions of the studied specimens are similar to those of *D. crassum* from Sansan (Morales et al., 2012), Thierhaupten (Seehuber, 2015), and Sandelzhausen (Rössner, 2010). Moreover, since our specimens are diagnosed bunoselenodont medium-sized *Dorcatherium* specimens (see Table 2) that lack a p1, we have every reason to attribute them to *D. crassum*. Moreover, the metatarsal bones of *D. crassum* described by Rössner (2010) and Morales et al. (2012) are similar in shape and size (see Table 3).

4.2. Intraspecific variability in D. crassum

We noticed some differences in the structure of the p4 in our set of specimens (Fig. 6). AP2014.0.129 possesses a p4 that is a little more derived with the presence of an anterior stylid, absent from the other specimens and from the specimens from Sansan (see figures in Morales et al., 2012). However, Aiglstorfer et al. (2014) and Mennecart (2015) already noticed that the p4 may be variable within populations in Tragulina (being more or less molarized, bearing additional cristids and folds) what corresponds to findings in other ruminants (Janis & Lister, 1985) and classical intraspecific variability. In our specimens, the differences may also be linked to difference in the preservation.

Rössner (2007) and Morales et al. (2012) proposed to use the fusion degree of the bones to better understand the evolution of Tragulidae. *Hyemoschus* possesses less fused hind limb bones than its Asian (and more derived; Mennecart & Costeur, 2016b; Sánchez et al., 2015) relatives (Rössner, 2007). Associated to dental characters, it has been proposed that *Dorcatherium* and *Hyemoschus* could be congeneric

(see in Gentry et al., 1999). However, Morales et al. (2012) noticed that the grade of fusion of the metatarsal bones varies a lot within the Sansan population. It ranges from unfused to well-fused (without noticeable bone suture) in adult specimens. So, this character should be taken with caution. The here described specimen AP2015.0128 is fully fused without any noticeable bone suture.

It is commonly admitted that the morphology of the ear region can be correlated with ecological and environmental parameters (e.g., Billet et al., 2012; Grohé et al., 2015; Pfaff et al., 2015). However, the bony labyrinth and ossicles are proven to fully ossify in foetuses long before birth at mid-gestation time in some ruminants (Costeur et al., 2016a, 2016b; Mennecart & Costeur, 2016a). In addition, the morphological intraspecific variability of the bony labyrinth, observed within Artiodactyla, is smaller than the interspecific morphological diversity and is thus highly conservative (Aguirre-Fernández et al., 2017; Mennecart & Costeur, 2016a). Thus, recent studies propose that the ear region supports a strong phylogenetic signal (Ekdale, 2013; Mennecart & Costeur, 2016b; Mennecart et al., 2016). The bony labyrinth of *D. crassum* described by Mennecart & Costeur (2016b, 2016c) is very similar to the specimen described here even if the shape and length of their common crus are different. Mennecart & Costeur (2016a) already noticed intraspecific variation of this structure in living Tragulidae. The height of the common crus may form a more or a less acute angle between the anterior and the posterior canal and accordingly influences the relative length of the vestibular aqueduct to the common crus height (Mennecart & Costeur, 2016a). Here we confirm the specific attribution of the isolated petrosal bone described by Mennecart & Costeur (2016b) to *D. crassum* and we demonstrate that the bony labyrinth can be used confidently for taxonomic purposes.

4.3. Skull heterochrony in Tragulidae

Developmental heterochrony is known in ruminant lineages. The development of the appendages in Cervidae due to social competition (hypermorphs, Geist, 1998) may be related to peramorphosis. Vrba et al. (1994) highlighted for an antelope lineage (Reduncini) that paedomorphosis (may be neoteny) affected cranial and reproductive characters and occurred together with an increase of the body size within the genus *Kobus*. Van der Geer (2005) suggested that insular artiodactyls that are exhibiting ancestral characters could be considered as paedomorphic dwarfs.

We noticed that *D. crassum* skull characters are similar to those of *Hyemoschus* (e.g., occipital condyles somewhat detached). However, the characters often are hyper-developed in *D. crassum*, while they are much less developed in *Tragulus* and *Moschiola*, *Hyemoschus* being intermediary (sagittal crest, nuchal crest, jugular process; see Table 4). It is interesting to note that these crests are also weaker in *Hyemoschus* juveniles and female. Life history characters in *Hyemoschus*, on the one hand, and in *Moschiola* plus *Tragulus*, on the other hand, are totally different. *Hyemoschus* weights two to eight times the weight of *Moschiola* and *Tragulus*. Moreover, the gestation time (ca. 150 days) and the sexual maturity (ca. 5 months) in *Moschiola* and *Tragulus* is very short in comparison to *Hyemoschus* (225 days and 18 months respectively; see Dubost et al., 2011, Table 4). Though, all three genera have a similar age at weaning (ca. 10 to 12 weeks) and a similar potential longevity (12–15 years).

Table 4
Summary of the potential heterochronic skull elements and life history (data from Dubost et al., 2011 for living tragulids and Rössner, 2010 for *Dorcatherium crassum* body weight).
Tableau 4
Résumé des éléments crâniens potentiellement hétérochroniques et stratégie de reproduction (données issues de Dubost et al., 2011 concernant les Tragulidae actuels et Rössner, 2010 pour le poids de *Dorcatherium crassum*).

	Dorcatherium	*Hyemoschus*	*Moschiola*	*Tragulus*
Supraorbital foram	++	–	–	–
Postorbital bar	++	–	–	–
Sagittal crest	++	+	–	–
Nuchal crest	++	+	–	–
Occipital condyles somewhat detached	+	+	–	–
Nuchal tubercules	++	–	–	–
Jugular processes	++	+	–	–
Gestation time (days)	?	225	150	154–140
Age at weaning (weeks)	?	12	?	10–11.5
Sexual maturity (months)	?	18	?	5.5–4.5
Longevity (years)	?	13	?	15–12
Bodymass (kg)	15	11	2.5	1–7

++: Well-marked character; +: marked character; –: absent character.

According to phylogenetic analyses (Mennecart & Costeur, 2016a, 2016b, 2016c; Sánchez et al., 2015), *Hyemoschus* is the sister group of the clade composed by *Tragulus* and *Moschiola*, while *Dorcatherium* is the sister taxon of the three living genera. Hence, above described differences between these taxa may indicate a paedomorphosis process, probably a progenesis, in development and in reproduction strategies during tragulid evolution. Body size reduction associated with progenesis may "have been selected for by high environmental unpredictability and might also be correlated with dietary changes in the small species" (Bärmann, 2014) that, in the case of tragulids, is based practically only on fruit (Heydon & Bolloh, 1997). Another explanation for the body size reduction is the diversification of the more efficient in fiber consumption Pecora groups that displaced to tragulids to niches in which a frugivorous diet is possible year-round (Clauss & Rössner, 2014).

4.4. Presence of Dorcatherium in the Faluns Formation

Dorcatherium is well-known to occur abundantly in the sediments of the Pontlevoy–Thenay Basin (Loir-et-Cher, France) from where *D. crassum* specimens have often been reported (e.g., Collier & Huin, 1977; Ginsburg & Mornand, 1986; Mayet, 1908; Stehlin, 1925). The Faluns Formation (Blaisois, Pontlevoy–Thenay Basin; Touraine, Savigné-sur-Lathan Basin) is mainly composed of marine sand deposits (Ginsburg, 2001; Ginsburg & Mornand, 1986) and famous for its paleontological content. No less than 58 species

of mammals indicating European Neogene Mammal Unit MN5 are currently known from the Faluns (Ginsburg, 2001; Ginsburg & Mornand, 1986), which are clearly distinct from older and reworked specimens (eroded, broken, darker colour), characteristic for MN2 ("calcaire de Beauce" Formation), MN3, and MN4 ("sable de l'Orléanais" formation), or even extremely rare dinosaur remains, which can be found there as well (Buffetaut & Pouit, 1994; Ginsburg, 2001). Of the MN5 mammal community, *Dorcatherium* is particularly well-documented in the Faluns deposits. In 1925, Stehlin already reported on specimens of *D. crassum*, *D. guntianum*, and *D. rogeri* (= *D. vindobonense*) in the Bourgeois collection (Pontlevoy, Pontlevoy–Thenay Basin) and Ginsburg (2001) on *D. crassum*, *D. guntianum*, and *D. peneckei* in the Basin of Savigné-sur-Lathan. However, until now, no skull was known.

These data match the evidence from other European sites that *D. crassum* and *D. guntianum*, appear in Europe within MN4 during late Burdigalian (late early Miocene), and that *D. peneckei*, and *D. vindobonense* appear in Europe with MN5 during Langhian (early middle Miocene) (Aiglstorfer et al., 2014; Rössner, 2017; Rössner & Heissig, 2013). Oddly, the presence of *D. naui* in the Faluns from Touraine and Blaisois (Langhian) was proposed based on a unique isolated tooth (Gagnaison et al., 2012) or in faunal lists (Gagnaison, 2013; Gagnaison et al., 2009). This is in conflict with data from the rest of Europe, that document that *D. naui* appeared in Europe not earlier than the Serravalian, within MN7 (Aiglstorfer et al., 2014), i.e. 3 million years later than *D. crassum*. Ginsburg (2001) also published faunal lists from the same localities. It is interesting to note that there is no referring to *D. naui*, but instead *D. guntianum* is listed (Ginsburg, 2001). Moreover, the isolated m3 attributed to *D. naui* from the falunière de Tourelet has the "morphological characteristics of *Dorcatherium guntianum*" (Gagnaison et al., 2012), being crescentic. Both species belong to the selenodont *Dorcatherium* morphotype. However the size of the tooth is too small to belong to *D. naui* (12.9 × 7.3 mm) and falls in the range of *D. guntianum* observed by Aiglstorfer et al. (2014). Thus, we suppose that the *D. naui* specimens reported on by Gagnaison in his several studies correspond to *D. guntianum*. Yet, Ginsburg & Mornand (1986) described and illustrated specimens of *D.* cf. *naui* in younger Faluns deposits. Indeed, a second transgressive event is registered in the Doué-la-Fontaine Basin dated to MN9 (Vallesian) where these fossils were found.

It is noteworthy that the other *Dorcatherium* specimens from the falunière de Tourelet (Gagnaison et al., 2012), that are attributed to *D. guntianum*, are too big to belong to this species and the proportions do not correspond to tragulid lower molars (m1 28.0 × 24.0 mm and m2 22.0 × 25.0 mm).

5. Conclusion

This is the first description of a fossil tragulid skull found in a French locality. It provides access to internal skull structures which are associated with reliably systematically assignable dental remains in a fossil tragulid for the first time. The description of the internal morphology of the ear region corresponds to Mennecart & Costeur (2016b) description of an isolated petrosal bone from the Sansan site to *D. crassum*. Hence, our work supports that the bony labyrinth solely can be used confidently for systematic classification at species level. The well-preserved material also sheds light on the intraspecific variability (teeth and bony labyrinth) within a fossil tragulid species and population. The p4 complexity, as well as the common crus of the bony labyrinth, may vary.

Acknowledgements

All our gratitude goes to Mr. Perceval, the owner of the field, who kindly gave all the authorizations for digging. Furthermore, we thank the three reviewers (Maeva Orliac, Manuela Aiglstorfer, and Reviewer3) as well as the editor Lorenzo Rook for their very helpful comments, which largely improved the manuscript. The Swiss National Foundation is warmly thanked for granting the SNF Projects 200021_159854/1, P300P2_161065, and P3P3P2_161066.

References

Aguirre-Fernández, G., Mennecart, B., Sánchez-Villagra, M.R., Sánchez, R., Costeur, L., 2017. A fossil dolphin ear bone from the northern Neotropics, insights into habitat transitions in iniid evolution. J. Vert. Paleontol., http://dx.doi.org/10.1080/02724634.2017.1315817, e1315817.

Aiglstorfer, M., Rössner, G.E., Böhme, M., 2014. *Dorcatherium naui* and pecoran ruminants from the late Middle Miocene Gratkorn locality (Austria). Palaeobiodivers. Palaeoenviron. 94, 83–123.

Alba, D.A., Moyà-Solà, S., Robles, J.M., Casanovas-Vilar, I., Rotgers, C., Carmona, R., Galindo, J., 2011. Middle Miocene tragulid remains from Abocador de Can Mata: the earliest record of *Dorcatherium naui* from Western Europe. Geobios 44, 135–150.

Bärmann, E.V., 2014. The evolution of body size, horn shape and social behavior in crown Antilopini – an ancestral character state analysis. Zitteliana B 32, 185–196.

Bärmann, E.V., Rössner, G.E., 2011. Dental nomenclature in Ruminantia: Towards a standard terminological framework. Mamm. Biol. 76 (6), 762–768.

Baron, R., 1999. Anatomie comparée des mammifères domestiques : Tome 1. Ostéologie, 4e ed. Vigot, Paris, 761 p.

Billet, G., Hautier, L., Asher, R.J., Schwarz, C., Crumpton, N., Martin, T., Ruf, I., 2012. High morphological variation of vestibular system accompanies slow and infrequent locomotion in three-toed sloths. Proc. R. Soc. B 279, 3932–3939.

Boas, J.E., 1890. Zur Morphologie des Magens der Cameliden und Traguliden und über die systematische Stellung letzterer Abtheilung. Morphol. Jahrb. 16, 494–524.

Buffetaut, E., Pouit, D., 1994. Dinosaur and crocodilian remains from the Upper Cretaceous of west-central France. C. R. Acad. Sci. Paris Ser. II 319 (2), 253–259.

Castillo, L., Gagnaison, C., Grugier, O., Renou, J.-C., 2006. Étude paléoécologique du site miocène de Contres (L.-et-Cher, France). Bull. Soc. Etudes Sci. d'Anjou XX, 61–78.

Clauss, M., Rössner, G.E., 2014. Old world ruminant morphophysiology, life history, and fossil record: exploring key innovations of a diversification sequence. Acta Zool. Fenn. 51, 80–94.

Collier, A., Huin, J., 1977. Nouvelles données sur la faune de mammifères miocènes du bassin de Thenay-Pontlevoy (Loir-et-Cher, France). Bull. Soc. Hist. Nat. Toulouse 113 (1–2), 219–233.

Costeur, L., 2014. The petrosal bone and inner ear of *Micromeryx flourensianus* (Artiodactyla, Moschidae) and inferred potential for ruminant phylogenetics. Zitteliana B 32, 1–16.

Costeur, L., Mennecart, B., Schulz, G., Müller, B., 2016a. Prenatal growth stages show the development of the ruminant bony labyrinth and petrosal bone. J. Anat. 230 (2), 347–353, http://dx.doi.org/10.1111/joa.12549.

Costeur, L., Mennecart, B., Schulz, G., Müller, B., 2016b. Middle ear bones of a mid-gestation ruminant foetus extracted from X-ray computed tomography Proc. SPIE 9967, 99671Q-2.

Costeur, L., Schulz, G., Müller, B., 2014. High-resolution X-ray computed tomography to understand ruminant phylogeny. Proc. SPIE 9212, 921216-1-921216-7.
Dubied, M., Gilbert, C., Deleglise, M., Laurens, F., Mennecart, B., 2017. De l'importance de la collection Quatrehomme (Musée La Monnaye, Meung-sur-Loire) dans le paysage paléontologique français. Carnets Geol. 17 (5), 129–138, http://dx.doi.org/10.4267/2042/62541.
Dubost, G., Charron, F., Courcoul, A., Rodier, A., 2011. The Chinese water deer, *Hydropotes inermis* – A fast-growing and productive ruminant. Mamm. Biol. 76, 190–195.
Ekdale, E.G., 2013. Comparative anatomy of the bony labyrinth (inner ear) of placental mammals. Plos One 8, e66624.
Fahlbusch, V., 1985. Säugerreste (*Dorcatherium* Steneofiber) aus der miozänen Braunkohle von Wackersdorf/Oberpfalz. Mitt. Bayer. Staatssaml. Paläont. Hist. Geol. 25, 81–94.
Gagnaison, C., 2013. Les assemblages de vertébrés dans deux sites paléontologiques du bassin miocène de Savigné-sur-Lathan/Noyant-sous-le-Lude : La Guimardière et Pelmer (Maine-et-Loire, France). Geodiversitas 35 (1), 67–103.
Gagnaison, C., Castillo, L., Grugier, O., Renou, J.-C., 2006. Une hémimandibule de *Pliopithecus piveteaui* dans le Miocène de Contres (41 France). Symbiose nouvelle série 16, 26–29.
Gagnaison, C., Gagnaison, J.-C., Hartmann, J.-P., 2009. Les fossiles de mammifères miocènes de la collection J.-P. Hartmann conservées dans le Musée du Savignéen. Symbiose nouvelle série 23, 1–16.
Gagnaison, C., Guevel, B., Xerri, S., Sicot, J.-L., Villeneuve, J.-M., Cossard, B., 2012. La falunière du Tourrelet (Thenay, Loir-et-Cher, France) : nouvelles données sur les vertébrés des sables continentaux du Miocène moyen (Orléanien supérieur : MN5). Rev. Paleobiol. 31 (1), 219–234.
Geist, V., 1998. Deer of the world their evolution, behaviour, and ecology. Stackpole Books, Mechanicsburg, 421 p.
Gentry, A.W., Rössner, G.E., Heizmann, G.E.E.P.J., 1999. Suborder Ruminantia. In: Rössner, G.E., Heissig, K. (Eds.), The Miocene land mammals of Europe. Verlag Dr. Friedrich Pfeil, München, pp. 225–258.
Ginsburg, L., 2001. Les mammifères terrestres du Miocène moyen des Faluns du bassin de Savigné-sur-Lathan (France). Geodiversitas 23 (3), 381–394.
Ginsburg, L., Mornand, J., 1986. Les restes mammifères des faluns de l'Anjou-Touraine. Mém. Soc. Études Sci. Anjou 6, 1–18.
Grohé, C., Tseng, Z.J., Lebrun, R., Boistel, R., Flynn, J.J., 2015. Bony labyrinth shape variation in extant Carnivora: a case study of Musteloidea. J. Anat. 228 (3), 366–383, http://dx.doi.org/10.1111/joa.12421.
Hassanin, A., Delsuc, F., Ropiquet, A., Hammer, C., Jansen van Vuuren, B., Matthee, C., Ruiz-Garcia, M., Catzeflis, F., Areskoug, V., Thanh Nguyen, T., Coloux, A., 2012. Pattern and timing of diversification of Cetartiodactyla (Mammalia, Laurasiatheria), as revealed by a comprehensive analysis of mitochondrial genomes. C. R. Biologies 335, 32–50.
Heydon, M., Bolloh, P., 1997. Mousedeer densities in a tropical rainforest: the impact of selective logging. J. Appl. Ecol. 34, 484–496.
Janis, C.M., Lister, A., 1985. The morphology of the lower fourth premolar as a taxonomic character in the Ruminantia (Mammalia, Artiodactyla), and the systematic position of Triceromeryx. J. Palaeontol. 59 (2), 405–410.
Kaup, J.J., 1839. Description d'ossements fossiles de Mammifères inconnus jusqu'à présent, qui se trouvent au Muséum grand-ducal de Darmstadt, cinquième cahier. J.P. Diehl, Darmstadt.
Köhler, M., 1993. Skeleton and habitat of recent and fossil ruminants. Münchner Geowiss. Abh. Geol. Paläont. 25, 1–88.
Kostopoulos, D.S., Sen, S., 2016. In: Sen, S. (Ed.), Suidae, Tragulidae, Giraffidae, and Bovidae, Late Miocene mammal locality of Küçükçekmece, European Turkey. Geodiversitas 38 (2), 273–298.
Mayet, L., 1908. Étude des mammifères miocènes des sables de l'Orléanais et des faluns de la Touraine. Ann. Univ. Lyon 24, 1–85.
Mennecart, B., 2012. The Ruminantia (Mammalia, Cetartiodactyla) from the Oligocene to the early Miocene of Western Europe: systematics, palaeoecology and palaeobiogeography. Geofocus 32, 1–263.
Mennecart, B., 2015. The European ruminants during the "*Microbunodon* Event" (MP28, latest Oligocene): impact of climate changes and faunal event on the ruminant evolution. Plos One 10 (2), e0116830.
Mennecart, B., Becker, D., Berger, J.-P., 2011. *Iberomeryx minor* (Mammalia, Artiodactyla) from the early Oligocene of Soulce (Canton Jura, NW Switzerland): systematics and palaeodiet. Swiss J. Geosci. 104 (Suppl. 1), S115–S132.
Mennecart, B., Costeur, L., 2016a. Shape variation and ontogeny of the ruminant bony labyrinth, an example in Tragulidae. J. Anat. 229 (3), 422–435, http://dx.doi.org/10.1111/joa.12487.
Mennecart, B., Costeur, L., 2016b. A *Dorcatherium* (Mammalia, Ruminantia, Middle Miocene) petrosal bone and the tragulid ear region. J. Vert. Paleontol., http://dx.doi.org/10.1080/02724634.2016.1211665.
Mennecart, B., Costeur, L., 2016c. 3D models related to the publication: a *Dorcatherium* (Mammalia, Ruminantia, middle Miocene) petrosal bone and the tragulid ear region. MorphoMuseuM 2, http://dx.doi.org/10.18563/m3.2.1.e2 (1)-e2.
Mennecart, B., Métais, G., 2015. *Mosaicomeryx* gen. nov., a ruminant mammal from the Oligocene of Europe and the significance of "gelocids". J. Syst. Palaeontol. 13, 581–600.
Mennecart, B., de Perthuis, A., Costeur, L., 2017. 3D models related to the publication: The first French tragulid skull (Mammalia, Ruminantia, Tragulidae) and associated tragulid remains from the Middle Miocene of Contres (Loir-et-Cher, France). MorphoMuseuM 3, http://dx.doi.org/10.18563/m3.3.3.e4 (3)-e4.
Mennecart, B., Rössner, G.E., Métais, G., DeMiguel, D., Schultz, G., Müller, B., Costeur, L., 2016. The petrosal and bony labyrinth of Early to Middle Miocene European deer (Mammalia, Cervidae) reveal their phylogeny. J. Morphol. 277, 1329–1338.
Métais, G., Vislobokova, I., 2007. Basal ruminants. In: Prothero, D.R., Foss, S.C. (Eds.), The evolution of artiodactyls. The Johns Hopkins University Press, Baltimore, pp. 189–212.
Métais, G., Chaimanee, Y., Jaeger, J.-J., Ducrocq, S., 2001. New remains of primitive ruminants from Thailand: evidence of the early evolution of the Ruminantia in Asia. Zool. Scripta 30, 231–249.
Milne-Edwards, A., 1864. Recherches anatomiques, zoologiques et paléontologiques sur la famille des chevrotains. Ann. Sci. Nat. Paris 5, 49–167.
Morales, J., Sánchez, I.M., Quiralte, V., 2012. Les Tragulidae (Artiodactyla) de Sansan. In: Peigné, S., Sen, S. (Eds.), Mammifères de Sansan., 203. Mémoires du Muséum national d'Histoire naturelle, Paris, pp. 225–247.
Mottl, M., 1961. Die Dorcatherien (Zwerghirsche) der Steiermark. Mitt. Mus. Bergbau Geol. Techn. Landesmus. Joanneum 22, 21–71.
Nowak, R.M., 1999. Walker's mammals of the world. The Johns Hopkins University Press, Baltimore and London, 1936 p.
O'Leary, M.A., 2010. An anatomical and phylogenetic study of the osteology of the petrosal of extant and extinct artiodactylans (Mammalia) and relatives. Bull. Am. Mus. Nat. His. 335, 1–206.
Pfaff, C., Matin, T., Ruf, I., 2015. Bony labyrinth morphometry indicates locomotor adaptations in the squirrel-related clade (Rodentia, Mammalia). Proc. R. Soc. B 282, 20150744.
Rössner, G.E., 2007. Tragulidae. In: Prothero, D.R., Foss, S.C. (Eds.), The evolution of artiodactyls. The Johns Hopkins University Press, Baltimore, pp. 213–220.
Rössner, G.E., 2010. Systematics and palaeoecology of Ruminantia (Artiodactyla, Mammalia) from the Miocene of Sandelzhausen (southern Germany, Northern Alpine Foreland Basin). Paläont. Z. 84, 123–162.
Rössner, G.E., 2017. New palaeontological and geological age constraints for the arrival and dispersal of Miocene tragulids (Tragulidae, Artiodactyla) in Europe. Zitteliana 89, 351–359.
Rössner, G.E., Heissig, K., 2013. New records of *Dorcatherium guntianum* (Tragulidae), stratigraphical framework, and diphyletic origin of Miocene European tragulids. Swiss J. Geosci. 106, 335–347.
Sánchez, I.M., Quiralte, V., Morales, M., Pickford, M., 2010. A new genus of tragulid ruminant from the early Miocene of Kenya. Acta Palaeontol. Pol. 55, 177–187.
Sánchez, I.M., Quiralte, V., Rios, M., Morales, J., Pickford, M., 2015. First African record of the Miocene Asian mouse-deer *Siamotragulus* (Mammalia, Ruminantia, Tragulidae): implications for the phylogeny and evolutionary history of the advanced selenodont tragulids. J. Syst. Palaeontol. 13, 543–556.
Seehuber, U., 2015. Ein Schädelfund von *Dorcatherium crassum* (Lartet, 1851) aus der Oberen Süßwassermolasse bei Thierhaupten (Landkreis Augsburg, Bayern, Deutschland). Doc. Nat. 196 (2), 41–61.
Smit-van Dort, M., 1989. Skin, skull and skeleton characters of the mouse deer (Mammalia, Tragulidae), with keys to the species. Bull. Zoöl. Mus. Amsterdam 12 (5), 89–95.
Stehlin, H.G., 1925. Catalogue des ossements de Mammifères tertiaires de la collection Bourgeois à l'école de Pontlevoy (Loir.et.Cher). Bull. Soc. Hist. Nat. Anthr. Loir-et-Cher 18, 77–277.
Van der Geer, A.A.E., 2005. Island ruminants and parallel evolution of functional structures. Quat. hors-série 2, 231–240.
Van der Made, J., 1996. Pre-Pleistocene Land Mammals from Crete. In: Reese, D.S. (Ed.), Pleistocene and Holocene Fauna of Crete and Its First Settlers. Prehistory Press, Madison, pp. 69–79.
Vrba, E.S., Vaisnys, J.R., Gatesy, J.E., DeSalle, R., Wei, K.-Y., 1994. Analysis of paedomorphosis using allometric characters: the example of Reduncini (Bovidae, Mammalia). Syst. Biol. 43 (1), 92–116.